

A Stochastic Quasi-Newton Method for Large-Scale Optimization

R. H. Byrd* S.L. Hansen[†] Jorge Nocedal[‡] Y. Singer[§]

March 31, 2018

Abstract

The question of how to incorporate curvature information in stochastic approximation methods is challenging. The direct application of classical quasi-Newton updating techniques for deterministic optimization leads to noisy curvature estimates that have harmful effects on the robustness of the iteration. In this paper, we propose a stochastic quasi-Newton method that is efficient, robust and scalable. It employs the classical BFGS update formula in its limited memory form, and is based on the observation that it is beneficial to collect curvature information pointwise, and at regular intervals, through (sub-sampled) Hessian-vector products. This technique differs from the classical approach that would compute differences of gradients, and where controlling the quality of the curvature estimates can be difficult. We present numerical results on problems arising in machine learning that suggest that the proposed method shows much promise.

*Department of Computer Science, University of Colorado, Boulder, CO, USA. This author was supported by National Science Foundation grant DMS-1216554 and Department of Energy grant de-sc0001774.

[†]Department of Engineering Sciences and Applied Mathematics, Northwestern University, Evanston, IL, USA. This author was supported by National Science Foundation grant DMS-0810213.

[‡]Department of Industrial Engineering and Management Sciences, Northwestern University, Evanston, IL, USA. This author was supported by National Science Foundation grant DMS-0810213, and by Department of Energy grant DE-FG02-87ER25047.

[§]Google Research

1 Introduction

Real world machine learning algorithms often construct very large models from massive amounts of training data. Learning complex models in this setting provides great opportunities for building highly accurate prediction models. However, the scale of these problems also imposes high computational and memory demands on the optimization algorithms employed to learn the models. In some applications, a full-batch (sample average approximation) approach is feasible and appropriate. However, in most large scale learning problems, it is imperative to employ stochastic approximation techniques that update the prediction model based on a relatively small subset of the training data. Stochastic approximation methods are particularly suited for settings where data is perpetually streamed to the learning process; examples include computer network traffic, web search, online advertisement, and sensor networks [10].

The goal of this paper is to propose a quasi-Newton method that operates in the stochastic approximation regime. We employ the well known limited memory BFGS updating formula [12], and show how to collect second-order information that is reliable enough to produce stable and productive Hessian approximations. The key is to compute average curvature estimates at regular intervals using (sub-sampled) Hessian-vector products. This ensures sample uniformity and avoids the potentially harmful effects of differencing noisy gradients.

The problem under consideration is the minimization of a convex stochastic function,

$$\min_{w \in \mathbb{R}^n} F(w) = \mathbb{E}[f(w; \xi)], \quad (1.1)$$

where ξ is a random variable. Although problem (1.1) arises other in settings, such as simulation optimization [2], we assume for concreteness that ξ is a random instance consisting of an input-output pair (x, z) . The vector x is typically referred to in machine learning as the input representation while z as the target output. In this setting, f typically takes the following form

$$f(w; \xi) = f(w; x_i, z_i) = \ell(h(w; x_i); z_i), \quad (1.2)$$

where ℓ is a loss function into \mathbb{R}_+ and h is a prediction model, parametrized by w . The collection of input-output pairs $\{(x_i, z_i)\}$, $i = 1, \dots, N$ is often referred to as the training set. The objective function (1.1) is defined using the empirical expectation

$$F(w) = \frac{1}{N} \sum_{i=1}^N f(w; x_i, z_i). \quad (1.3)$$

In learning applications with massive amounts for training data, it is often mandatory to use a stochastic gradient based on $b \stackrel{\Delta}{=} |\mathcal{S}| \ll N$ input-output instances, yielding

the following estimate

$$\widehat{\nabla}F(w) = \frac{1}{b} \sum_{i \in \mathcal{S}} \nabla f(w; x_i, z_i) . \quad (1.4)$$

The subset $\mathcal{S} \subset \{1, 2, \dots, N\}$ is randomly chosen, with b sufficiently small so that the algorithm operates in the stochastic approximation regime. Therefore, the stochastic estimates of the gradient are substantially faster to compute than a gradient based on the entire training set.

Our optimization paradigm employs iterations of the form

$$w^{k+1} = w^k - \alpha^k B_k^{-1} \widehat{\nabla}F(w^k) , \quad (1.5)$$

where B_k is a symmetric positive definite approximation to the Hessian matrix $\nabla^2 F(w)$, and $\alpha^k > 0$. In our experiments, the steplength parameter α^k has the form $\alpha^k = \beta/k$, where $\beta > 0$ is given, but other choices can be employed.

A critical question is how to construct B_k in a stable manner. Furthermore, to make each iteration scalable, the algorithm must be able to update the inverse matrix $H_k = B_k^{-1}$ directly, so that (1.5) can be implemented as

$$w^{k+1} = w^k - \alpha^k H_k \widehat{\nabla}F(w^k). \quad (1.6)$$

This step computation should require only $O(n)$ operations, as in limited memory quasi-Newton methods for deterministic optimization.

If we set $H_k = I$ and $\alpha^k = \beta/k$ in (1.6), we recover the classical Robbins-Monro method [20], which is also called the *stochastic gradient descent method*. Under standard assumptions, the number of iterations needed by this method to compute an ϵ -accurate solution is

$$\frac{\nu \kappa^2}{\epsilon} + O\left(\frac{1}{\epsilon}\right),$$

where κ is the condition number of the Hessian at the optimal solution, $\nabla^2 F(w^*)$, and ν is a parameter that depends on both the Hessian matrix and the gradient covariance matrix; see [15, 5]. Therefore, the stochastic gradient descent method is adversely affected by ill conditioning in the Hessian. In contrast, it is shown by Murata [15] that setting $H_k = \nabla^2 F(w^*)^{-1}$ in (1.6) completely removes the dependency of κ from the complexity estimate. Although the choice $H_k = \nabla^2 F(w^*)^{-1}$ is not viable in practice, it suggests that an appropriate choice of H_k may result in an algorithm that improves upon the stochastic gradient descent method.

In the next section, we present a stochastic quasi-Newton method of the form (1.6) that is designed for large-scale applications. It employs the limited memory BFGS method, which is defined in terms of *correction pairs* (s, y) that provide an estimate of the curvature of the objective function $F(w)$ along the most recently generated directions. We propose a novel way of defining these correction pairs that yields

curvature estimates that are not corrupted by the effect of differencing the noise in the gradients. Our numerical experiments, using problems arising in machine learning, suggest that the new method is robust and efficient.

The paper is organized into 5 sections. The new algorithm is presented in section 2, and in section 3 we describe a set of experiments to illustrate its practical performance. A literature survey on related stochastic quasi-Newton methods is given in section 4. The paper concludes in section 5 with some remarks about the contributions of the paper, and with some open questions.

Notation. The terms Robbins-Monro method, stochastic approximation (SA) method, and stochastic gradient descent (SGD) method are used in the literature to denote (essentially) the same algorithm. The first term is common in statistics, the second term is popular in the stochastic programming literature, and the acronym SGD is standard in machine learning. We will use the name stochastic gradient descent method (SGD) in the discussion that follows.

2 A stochastic quasi-Newton method

The success of quasi-Newton methods for deterministic optimization lies in the fact that they construct curvature information during the course of the optimization process, and this information is good enough to endow the iteration with a superlinear rate of convergence. In the classical BFGS method [9] for minimizing a function $F(w)$, the new inverse approximation H_{k+1} is uniquely determined by the previous approximation H_k and the correction pairs

$$y = \nabla F(w^{k+1}) - \nabla F(w^k), \quad s = w^{k+1} - w^k.$$

The BFGS update is well defined as long as the curvature condition $y^T s > 0$ is satisfied, which is always the case when $F(w)$ is strictly convex.

For large scale applications, it is necessary to employ a limited memory variant that is scalable in the number of variables, but enjoys only a linear rate of convergence. Nevertheless, this so called L-BFGS method [17] is considered generally superior to the steepest descent method for deterministic optimization: it produces well scaled and productive search directions that yield an approximate solution in fewer iterations and function evaluations.

2.1 A Preliminary Approach

There are various ways of trying to extend the concept of quasi-Newton updating for the minimization of the stochastic function (1.1). Here we attempt to follow the simplest approach, and explore the use of the BFGS formula.

The first observation is that it is not advisable to mimic classical quasi-Newton methods for deterministic optimization and update the model based on information from only one iteration. This is because quasi-Newton updating is inherently an overwriting process rather than an averaging process, and therefore the vector y must reflect the action of the Hessian of the entire objective F given in (1.1). Instead, we could employ a *collection* of gradients evaluated at iterates w^k .

This suggests the following naive approach that appears to be a natural adaptation of quasi-Newton updating. Suppose we are given two disjoint collections of iterates and their corresponding stochastic gradients,

$$\{(w^i, \widehat{\nabla}F(w^i)) \mid i \in I\}, \quad \{(w^j, \widehat{\nabla}F(w^j)) \mid j \in J\}, \quad (2.1)$$

and let us assume for simplicity that $|I| = |J| \triangleq L$. We then define the average iterate and average gradient for the collection I as

$$\bar{w}_I = \frac{1}{|I|} \sum_{i \in I} w^i, \quad \bar{g}_I = \frac{1}{|I|} \sum_{i \in I} \widehat{\nabla}F(w^i), \quad (2.2)$$

and define \bar{w}_J and \bar{g}_J similarly. Given these two pairs of average iterates and gradients, the correction vectors to be used in BFGS updating would be defined as

$$\bar{y} = \bar{g}_I - \bar{g}_J, \quad \bar{s} = \bar{w}_I - \bar{w}_J. \quad (2.3)$$

This information allows us to apply the BFGS update formula using $\{\bar{s}, \bar{y}\}$, assuming that the curvature condition $\bar{s}^T \bar{y} > 0$ holds.

The algorithm would proceed as follows. First, it runs the SGD iteration (i.e. (1.6) with $H_k = I$) until sufficient stochastic gradients have been computed to form the two collections (2.1) and the corresponding correction pairs (2.3). At this point a limited memory BFGS update is performed, using the correction pairs (2.3) to obtain the first quasi-Newton approximation H . The algorithm then performs L stochastic quasi-Newton iterations (1.6) with the (fixed) Hessian approximation H . After these L stochastic quasi-Newton iterations have been performed, we redefine the sets (2.1) so that I contains the most recently computed iterates and stochastic gradients, and J contains the previous L computed iterates and stochastic gradients. We use the redefined sets (2.1) to compute a new approximation H . The process is then repeated in this manner: every iteration is of the form (1.6), where the inverse Hessian approximation is updated every L iterations using the most recently collected pairs (2.3)

We found that this method was *not successful* in practice. We applied it to the learning problems described in section 3 and observed that the iteration (1.6) was neither faster nor more robust than the stochastic gradient descent method.

2.2 The stochastic BFGS method

The difficulties mentioned above are caused by the fact that, if the average gradients \bar{g}_I and \bar{g}_J are too noisy, the BFGS update (which is based on differences) will exacerbate the effect of the noise and yield a poor Hessian approximation. This results in an unstable iteration, as observed by [23, 13], and many other authors. Even if the average gradients \bar{g}_I and \bar{g}_J do not have high variance, the vector \bar{y} may be poor simply because the samples (x_i, z_i) used at those iterations that define the sets I and J are different. In other words, using averages of stochastic gradients to compute the curvature pair (2.3) can lead to high variance in \bar{y} due to two sources of error: the lack of sample uniformity just mentioned, and the harmful effects of sample variance in the gradients \bar{g}_I and \bar{g}_J , when computing differences. Both have adverse effects in quasi-Newton updating.

An effective way of removing the lack of sample uniformity is to compute \bar{y} via a Hessian-vector product; i.e., by approximating differences in gradients via a first order Taylor expansion:

$$\bar{y} = \bar{g}_I - \bar{g}_J \approx \widehat{\nabla}^2 F(\bar{w}_I) \bar{s}.$$

Let $\mathcal{S}_H \subset \{1, \dots, N\}$ be a small subset of the training examples and define

$$\widehat{\nabla}^2 F(w) \triangleq \frac{1}{b_H} \sum_{i \in \mathcal{S}_H} \nabla^2 f(w; x_i, z_i), \quad (2.4)$$

where b_H is the cardinality of \mathcal{S}_H . We maintain the idea of updating the BFGS Hessian using a collection of iterates, as discussed in section 2.1, but we replace the definition of the correction pairs (2.3) with

$$\bar{y} = \widehat{\nabla}^2 F(\bar{w}_I) \bar{s}, \quad \bar{s} = \bar{w}_I - \bar{w}_J. \quad (2.5)$$

We would like to emphasize that the matrix $\widehat{\nabla}^2 F(\bar{w}_I)$ is never constructed explicitly when computing \bar{y} in (2.5), rather, the Hessian-vector product can be coded directly. In addition, the sampled Hessian in (2.5) could be evaluated at w^k instead of \bar{w}_I , since the Hessian-vector products need only provide a general estimate of the curvature of the objective function. The pseudocode of the complete method is given in Algorithm 1.

Algorithm 1 Stochastic L-BFGS Method

Input: initial parameters w^0 , $M \in \mathbb{N}$, $L \in \mathbb{N}$, $K \in \mathbb{N}$, step-length sequence $\alpha^k \in (0, 1)$ **Output:** final weights w^K

- 1: Set $t = 0$ ▷ Records number of times Hessian has been updated
- 2: $\bar{w}_J = w^0$, $\bar{w}_I = 0$
- 3: **for** $k = 1, \dots, K - 1$ **do**
- 4: Calculate stochastic gradient $\widehat{\nabla}F(w^k)$
- 5: $\bar{w}_I = \bar{w}_I + w^k$
- 6: **if** $k < 2L$ **then**
- 7: $w^{k+1} = w^k - \alpha^k \widehat{\nabla}F(w^k)$ ▷ Stochastic gradient iteration
- 8: **else**
- 9: $w^{k+1} = w^k - \alpha^k H_t \widehat{\nabla}F(w^k)$ ▷ L-BFGS step computation with memory M
- 10: **end if**
- 11: **if** $\text{mod}(k, L) = 0$ **then** ▷ Compute correction pairs every L iterations
- 12: $t = t + 1$
- 13: $\bar{w}_I = \bar{w}_I / L$
- 14: Compute new curvature pairs:

$$\bar{s}_t = (\bar{w}_I - \bar{w}_J), \quad \bar{y}_t = \widehat{\nabla}^2 F(\bar{w}_I)(\bar{w}_I - \bar{w}_J)$$

- 15: $\bar{w}_J = \bar{w}_I$, $\bar{w}_I = 0$
 - 16: **end if**
 - 17: **end for**
 - 18: **return** w^K
-

The L-BFGS step computation in Step 9 follow standard practice [17]. The matrix H_t is the result of applying M BFGS updates to an initial matrix H_t^0 using the M most recent correction pairs $\{\bar{s}_j, \bar{y}_j\}_{j=t-M+1}^t$ computed by the algorithm. The matrix H_t is not formed explicitly, and to compute the product $H_t \widehat{\nabla}F(w^k)$ one employs a formula based on the structure of the 2-rank BFGS update. This formula is commonly called the two loop recursion, and is described in [17, §7.2]. The initial inverse Hessian approximation is given by,

$$H_t^0 = \theta I, \quad \theta_t = \frac{\bar{s}_t^T \bar{y}_t}{\bar{y}_t^T \bar{y}_t}, \quad (2.6)$$

where \bar{s}_t and \bar{y}_t are computed in Step 14.

We prefer our approach over a method that would enforce sample uniformity by using finite differences to define \bar{y} in (2.5), such as

$$\bar{y} = \widehat{\nabla}F(\bar{w}_I) - \widehat{\nabla}F(\bar{w}_J), \quad (2.7)$$

where the same sample \mathcal{S} is used in computing the stochastic gradients at \bar{w}_I and \bar{w}_J . This is because the Hessian-vector product approach is no more expensive, allows complete freedom in the choice of the sample \mathcal{S} at each iteration, and avoids finite differencing problems when $\|\bar{w}_I - \bar{w}_J\|$ is small.

In summary, the algorithm builds upon the strengths of BFGS updating, but deviates from the classical method in that the correction pairs (\bar{s}, \bar{y}) are based on average iterates and sub-sampled Hessian-vector products, respectively. Our task in the remainder of the paper is to argue that even with the extra computational cost of Hessian-vector products (2.5) and the extra cost of computing the iteration (1.6), the stochastic quasi-Newton method is competitive with the SGD method in terms of computing time (even in the early stages of the optimization), and is able to find a lower objective value.

2.3 Cost of the stochastic BFGS method

Let us compare the cost of the stochastic gradient descent method

$$w^{k+1} = w^k - \frac{\beta}{k} \widehat{\nabla} F(w^k) \quad (\text{SGD}) \quad (2.8)$$

and the stochastic quasi-Newton method

$$w^{k+1} = w^k - \frac{\beta}{k} H_t \widehat{\nabla} F(w^k) \quad (\text{SQN}) \quad (2.9)$$

given by Algorithm 1.

The quasi-Newton matrix-vector product in (2.9) requires approximately $4Mn$ operations [17]. To measure the cost of the gradient and Hessian-vector computations, let us consider one particular but representative example, namely the binary classification test problem tested in section 3; see (3.1). In this case, the component function f in (1.2) is given by

$$f(w; x_i, z_i) = z_i \log(c(w; x_i)) + (1 - z_i) \log(1 - c(w; x_i))$$

where

$$c(w; x_i) = \frac{1}{1 + \exp(-x_i^T w)}, \quad x_i \in \mathbb{R}^n, \quad w \in \mathbb{R}^n, \quad z_i \in \{0, 1\}. \quad (2.10)$$

The gradient and Hessian-vector product of f are given by,

$$\nabla f(w; x_i, z_i) = (c(w; x_i) - z_i)x_i \quad (2.11)$$

$$\nabla^2 f(w; x_i, z_i)\bar{s} = c(w; x_i)(1 - (c(w; x_i))(x_i^T \bar{s}))x_i. \quad (2.12)$$

The evaluation of the function $c(w; x_i)$ requires approximately n operations (where we follow the convention of counting a multiplication and an addition as an operation).

Therefore, by (2.11) the cost of evaluating one batch gradient is approximately $2bn$, and the cost of computing the Hessian-vector product $\widehat{\nabla}^2 F(\bar{w}_I)\bar{s}$ is about $3b_H n$. This assumes these two vectors are computed independently. If the Hessian is computed at the same point where we compute a gradient and $b \geq b_H$ then $c(w; x_i)$ can be reused for a savings of $b_H n$.

Therefore, for binary logistic problems the total number of floating point operations of the stochastic quasi-Newton iteration (2.9) is approximately

$$2bn + 4Mn + 3b_H n/L. \quad (2.13)$$

On the other hand, the cost associated with the computation of the SGD step is only bn . At first glance it may appear that the SQN method is prohibitively expensive, but this is not the case when using the values for b , b_H , L and M suggested in this paper. To see this, note that

$$\frac{\text{cost of SQN iteration}}{\text{cost of SGD iteration}} = 1 + \frac{2M}{b} + \frac{2b_H}{3bL}. \quad (2.14)$$

In the experiments reported below, we use $M = 5$, $b = 50, 100, \dots$, $L = 10$ or 20 , and choose b_H to be of similar magnitude as b . For such parameter settings, the additional cost of the SQN iteration is small relative to the cost of the SGD method.

For the multiclass logistic regression problem described in section 3.3, the costs of gradient and Hessian-vector products are slightly different. Nevertheless, the relative cost of the SQN and SGD iterations is similar to that given in (2.14).

The quasi-Newton method can take advantage of parallelism. Instead of employing the two-loop recursion mentioned above to implement the limited memory BFGS step computation in step 9 of Algorithm 1, we can employ the compact form of limited memory BFGS updating [17, §7.2] in which H_t is represented as the outer product of two matrices. This computation can be parallelized and its effective cost is around $3n$ operations, which is smaller than the $4Mn$ operations assumed above. The precise cost of parallelizing the compact form computation depends on the computer architecture, but is in any case independent of M .

Additionally, the Hessian-vector products can be computed in parallel with the main iteration (2.9) if we allow freedom in the choice of the point \bar{w}_I where (2.5) is computed. The choice of this point is not delicate since it suffices to estimate the average curvature of the problem around the current iterate, and hence the computation of (2.5) can lag behind the main iteration. In such a parallel setting, the computational overhead of Hessian-vector products may be negligible.

3 Numerical Experiments

In this section, we compare the performance of the stochastic gradient descent method (2.8) and the stochastic quasi-Newton method (2.9) on three test problems of the form

(1.2)-(1.3) arising in supervised machine learning. The parameter $\beta > 0$ is fixed at the beginning of each run, as discussed below, and the SQN method is implemented as described in Algorithm 1.

It is well known amongst the optimization and machine learning communities that the SGD method can be improved by choosing the parameter β via a set of problem dependent heuristics [19, 25]. In some cases, β_k (rather than β) is made to vary during the course of the iteration, and could even be chosen so that β_k/k is constant, in which case only convergence to a neighborhood of the solution is guaranteed [16]. There is, however, no generally accepted rule for choosing β_k , so our testing approach is to consider the simple strategy of selecting the (constant) β so as to give good performance for each problem.

Specifically, in the experiments reported below, we tried several values for β in (2.8) and (2.9) and chose a value for which increasing or decreasing it by a fixed increment results in inferior performance. This allows us to observe the effect of the quasi-Newton Hessian approximation H_k in a controlled setting, without the clutter introduced by elaborate step length strategies for β_k .

In the figures provided below, we use the following notation.

1. n : the number of variables in the optimization problem; i.e., $w \in \mathbb{R}^n$.
2. N : the number of training points in the dataset.
3. b : size of the batch used in the computation of the stochastic gradient $\widehat{\nabla}F(w)$ defined in (1.4); i.e., $b = |\mathcal{S}|$.
4. b_H : size of the batch used in the computation of Hessian-vector products (2.5) and (2.4); i.e., $b_H = |\mathcal{S}_H|$.
5. L : controls the frequency with which the limited memory BFGS updating is performed, i.e., every L iterations a new curvature pair (2.5) is formed, the oldest pair is removed, and the new set of correction pairs is used in the two-loop recursion for calculating the quasi-Newton direction (Step 9 of Algorithm 1).
6. M : memory used in limited memory BFGS updating.
7. adp: Accessed data points. At each iteration the SGD method evaluates the stochastic gradient $\widehat{\nabla}f(w^k)$ using b randomly chosen training points (x_i, z_i) , so we say that the iteration accessed b data points. On the other hand, an iteration of the stochastic BFGS method accesses $b + b_H/L$ points.
8. iteration: In some graphs we compare SGD and SQN iteration by iteration (even though the cost of the SQN iteration is higher).

9. epoch: One complete pass through the dataset.

In our experiments, the stochastic gradient (1.4) is formed by randomly choosing b training points from the dataset without replacement. This process is repeated every epoch, which guarantees that all training points are equally used when forming the stochastic gradient. The same procedure is applied to the evaluation of the Hessian-vector products. Independent of the stochastic gradients, the Hessian-vector products are formed by randomly choosing b_H training points from the dataset without replacement.

3.1 Experiments with Synthetic Datasets

We first test our algorithm on a binary classification problem using randomly generated training points, as described in [14]. The objective function is given by

$$F(w) = -\frac{1}{N} \sum_{i=1}^N z_i \log(c(w; x_i)) + (1 - z_i) \log(1 - c(w; x_i)), \quad (3.1)$$

where $c(w; x_i)$ is given by (2.10).

We report results for a logistic regression problem using training points generated in the manner above with $N = 7000$ and $n = 50$. To establish a reference benchmark with a well known algorithm, we used the particular implementation of one of the coordinate descent (CD) methods in [24], as described in [14].

Figure 1 reports the performance of SGD (with $\beta = 7$) and SQN (with $\beta = 2$), as measured by either iteration count or accessed data points. Both methods use a gradient batch size of $b = 50$; for SQN we display results for two values of the Hessian batch size b_H , and set $M = 10$ and $L = 10$. The vertical axis, labeled \mathbf{fx} , measures the value of the objective (3.1); the dotted black line marks the best function value obtained by the coordinate descent (CD) method mentioned above. We observe that the SQN method with $b_H = 300$ and 600 outperforms SGD, and obtains the same or better objective value than the coordinate descent method. Figure 1 is consistent with the results we present below for more realistic datasets (RCV1 and SPEECH).

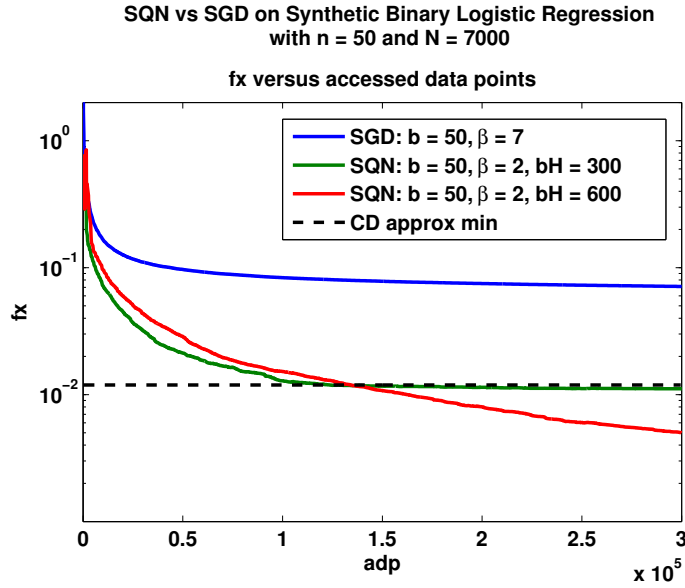


Figure 1: Illustration of SQN and SGD on the synthetic dataset. The dotted black line marks the best function value obtained by the coordinate descent (CD) method. For SQN we set $M = 10$, $L = 10$ and $b_H = 300$ or 600 (b_H stands for b_H).

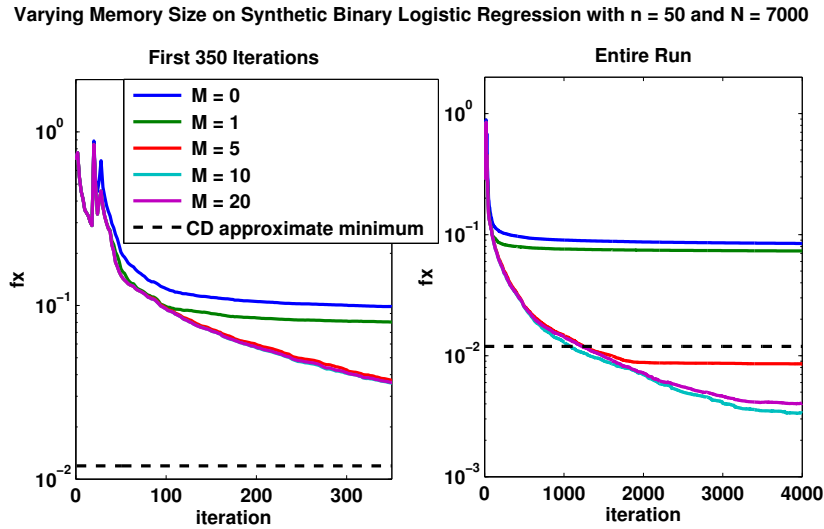


Figure 2: Effect of the memory size M in the SQN method. The figure on the left reports the first 4 epochs, while the figure on the right lets the algorithm run for more than 70 epochs to observe if the beneficial effect of increasing M is sustained. Parameters settings are $b = 50$, $b_H = 600$, and $L = 10$.

In Figure 2 we explore the effect of the limited memory size M . Increasing M beyond 1 and 2 steadily improves the performance of the SQN algorithm, both during the first few epochs (left figure), and after letting the algorithm run for many epochs (right figure). These results suggest that a larger memory size is helpful in the later stages of the run.

3.2 RCV1 Data Set

The RCV1 dataset [11] is a composition of newswire articles produced by Reuters from 1996-1997. Each article was manually labeled into 4 different classes: Corporate/Industrial, Economics, Government/Social, and Markets. For the purpose of classification, each article was then converted into a boolean feature vector with a 1 representing the appearance of a given word. Post word stemming, this gives each feature vector a dimension of $n = 112919$.

Each data point $x_i \in [0, 1]^n$ is extremely sparse, with an average of 91 (.013%) nonzero elements. There are $N = 688329$ training points. We consider the binary classification problem of predicting whether or not an article is in the fourth class, Markets, and accordingly we have labels $z_i \in \{0, 1\}$. We use logistic regression to model the problem, and define the objective function by equation (3.1).

In our numerical experiments with this problem, we used gradient batch sizes of $b = 50, 300$ or 1000 , which respectively comprise .0073%, .044% and .145% of the dataset. The frequency of quasi-Newton updates was set to $L = 20$, a value that balances the aims of quickly retrieving curvature information and minimizing computational costs. For the SGD method we chose $\beta = 5$ when $b = 50$, and $\beta = 10$ when $b = 300$ or 1000 ; for the SQN method (2.9) we chose $\beta = 1$ when $b = 50$, and $\beta = 5$ when $b = 300$ or 1000 .

Figure 3 reports the performance of the two methods as measured by either iteration count or accessed data points. As before, the vertical axis, labeled \mathbf{fx} , measures the value of the objective (3.1). Figure 3 shows that for each batch size b of 50, 300 or 1000, the SQN method outperforms SGD, and both methods improve as batch size increases. We observe that using a batch size b of 300 or 1000 yields different relative outcomes for the SQN method when measured in terms of iterations or adp: a batch size of 300 provides the fastest initial decrease in the objective, but that method is eventually overtaken by the variant with the larger batch size of 1000.

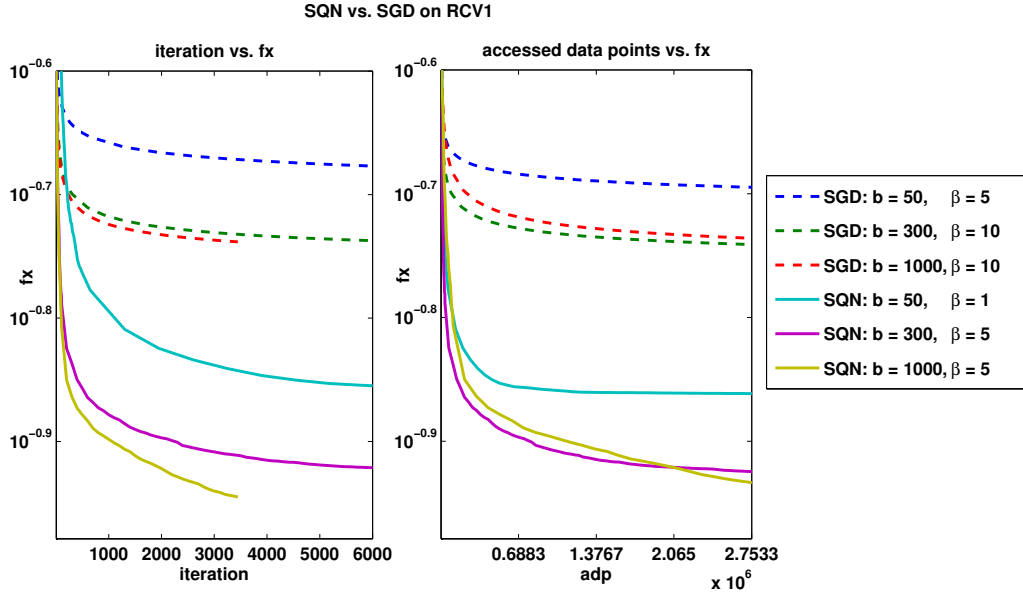


Figure 3: Illustration on RCV1 problem. For SGD and SQN, b is set to either 50, 300 or 1000, and for SQN we use $b_H = 1000$, $M = 5$, and $L = 20$. The figures report training error as a function of iteration count or accessed data points. In the rightmost graph the tick marks on the x-axis (at 0.6882, 1.3767, ...) denote the epochs of SGD.

Figure 4 illustrates the effect of varying the Hessian batch size b_H from 10 to 10000, while keeping the gradient batch size b fixed at 300 or 1000. For $b = 300$ (Figure 4a) increasing b_H improves the performance of SQN, in terms of adp, up until $b_H = 1000$, where the benefits of the additional accuracy in the Hessian approximation do not outweigh the additional computational cost. In contrast, Figure 4b shows that for $b = 1000$, a high value for b_H , such as 10000, can be effectively used since the cost of the Hessian-vector product relative to the gradient is lower. One of the conclusions drawn from this experiment is that there is much freedom in the choice of b_H , and that only a small subsample of the data (e.g. $b_H = 100$) is needed for the stochastic quasi-Newton approach to yield benefits.

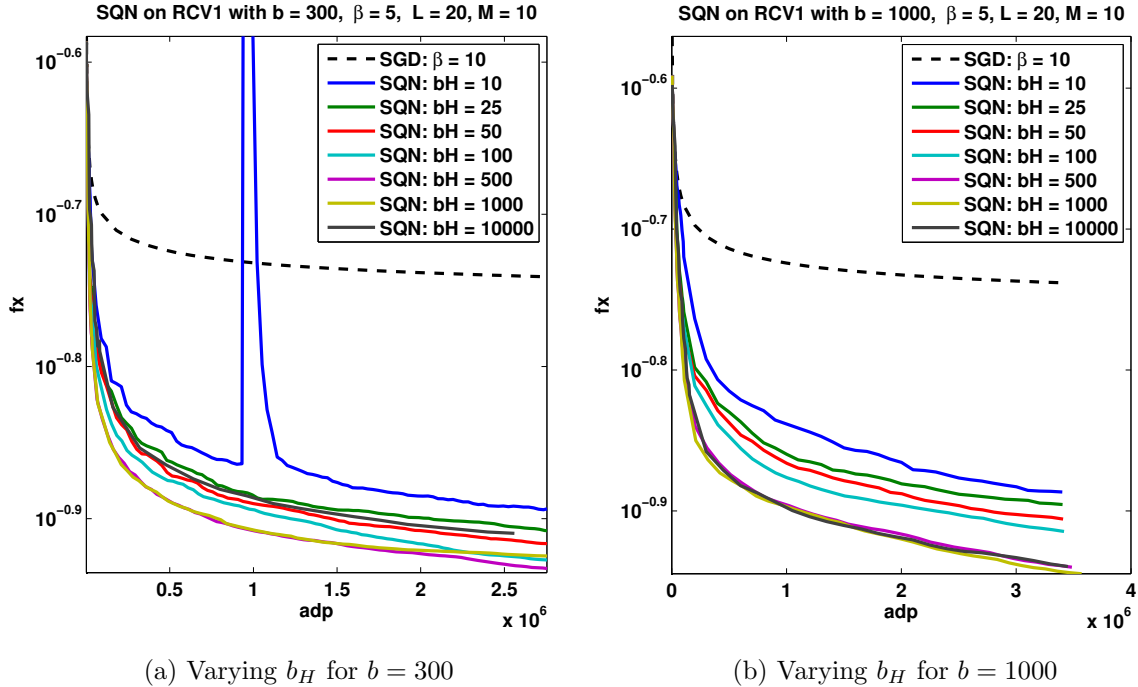


Figure 4: Varying Hessian batch size parameter b_H on the RCV1 dataset for gradient batch values b of 300 and 1000. All other parameters in the SQN method are held constant at $L = 20$, $M = 10$, and $\beta = 5$. Here b_H stands for b_H .

One should guard, however, against the use of very small values for b_H , as seen in the large blue spike in Figure 4a corresponding to $b_H = 10$. To understand this behavior, we monitored the angle between the vectors \bar{s} and \bar{y} and observed that it approached 90° between iteration 3100 and 3200, which is where the spike occurred. Since the term $\bar{s}^T \bar{y}$ enters in the denominator of the BFGS update formula for H_k [17, §7.2], this led to a very large and poor step. Monitoring $\bar{s}^T \bar{y}$ (relative to, say $\bar{s}^T B \bar{s}$) can be a useful indicator of a potentially harmful update; one can increase b_H or skip the update when this number is smaller than a given threshold.

The impact of the memory size parameter M is shown in Figure 5. The results improve consistently as M increases, but beyond $M = 2$ these improvements are rather small, especially in comparison to the results in Figure 2 for the synthetic data. The reasons for this difference are not clear, but for the deterministic L-BFGS method the effect of M on performance is known to be problem dependent. We observe that performance with a value of $M = 0$, which results in a Hessian approximation of the form $H_t = \theta_t I$ with θ_t given by (2.6), is poor and also unstable in early iterations, as shown by the spikes in Figure 5.

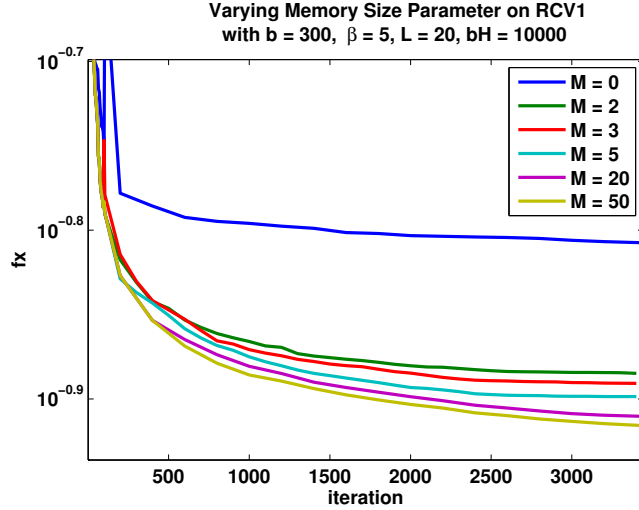


Figure 5: Impact of the memory size parameter on the RCV1 dataset. M is varied between 0 and 50 while all other parameters are held constant at $b = 300$, $L = 20$, and $b_H = 10000$.

To gain a better understanding of the behavior of the SQN method, we also monitored the following two errors:

$$\text{GradError} = \frac{\|\nabla F(w) - \widehat{\nabla} F(w)\|_2}{\|\nabla F(w)\|_2}, \quad (3.2)$$

and

$$\text{HvError} = \frac{\|\nabla^2 F(\bar{w}_I)(\bar{w}_I - \bar{w}_J) - \widehat{\nabla}^2 F(\bar{w}_I)(\bar{w}_I - \bar{w}_J)\|_2}{\|\nabla^2 F(\bar{w}_I)(\bar{w}_I - \bar{w}_J)\|_2}. \quad (3.3)$$

The quantities $\nabla F(w)$ and $\nabla^2 F(\bar{w}_I)(\bar{w}_I - \bar{w}_J)$ are computed with the entire data set, as indicated by (3.1). Therefore, the ratios above report the relative error in the stochastic gradient used in (2.9) and the relative error in the computation of the Hessian-vector product (2.5).

Figure 6 displays these relative errors for various batch sizes b and b_H , along with the norms of the stochastic gradients. These errors were calculated every 20 iterations during a *single run* of SQN with the following parameter settings: $b = 300$, $L = 20$, $M = 5$, and $b_H = 688329$. Batch sizes larger than $b = 10000$ exhibit non-stochastic behavior in the sense that all relative errors are less than one, and the norm of these approximate gradients decreases during the course of the iteration. Gradients with a batch size less than 10000 have relative errors greater than 1, and their norm does not exhibit decrease over the course of the run.

The leftmost figure also shows that the ℓ_2 norms of the stochastic gradients decrease as the batch size b increases, i.e., there is a tendency for inaccurate gradients to have a larger norm. This is because in a large sphere around a (true gradient) point near zero, most points in the sphere will have a larger ℓ_2 norm than the center.

Figure 6 indicates that the Hessian-vector errors stay relatively constant throughout the run and have smaller relative error than the gradient. As discussed above, some accuracy here is important while it is not needed for the batch gradient.

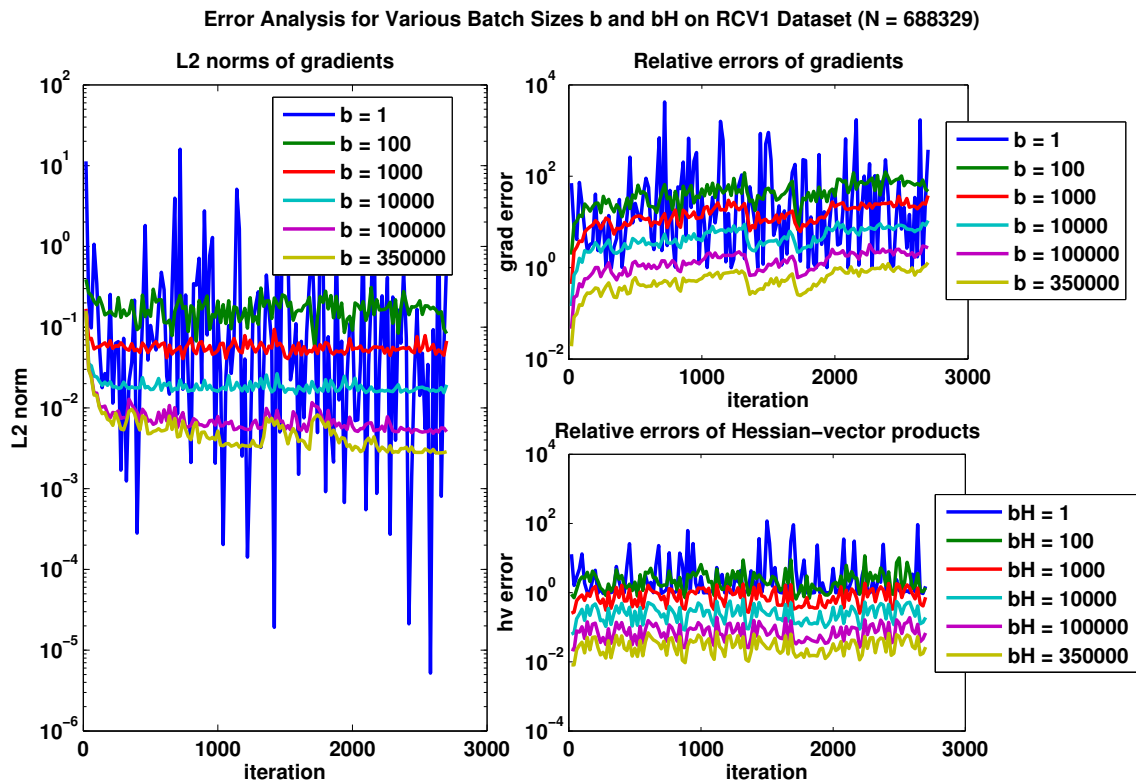


Figure 6: Error plots for RCV1 dataset. The figure on the left plots $\|\widehat{\nabla}F(w)\|_2$ for various values of b . The figures on the right display the errors (3.2) and (3.3). The errors were calculated every 20 iterations during a single run of SQN with parameters $b = 300$, $L = 20$, $M = 5$, and $b_H = \mathbf{bH} = 688329$.

3.3 A Speech Recognition Problem

The speech dataset, provided by Google, is a collection of feature vectors representing 10 millisecond frames of speech with a corresponding label representing the phonetic state assigned to that frame. Each feature x_i has a dimension of $NF = 235$ (the individual elements range from -7.0451 to 30.2266) and has corresponding label $z_i \in$

$C = \{1, 2, \dots, 129\}$. There are a total of $N = 191607$ samples; the number of variables is $n = NF \times |C| = 30315$.

The problem is modeled using multi-class logistic regression. The unknown parameters are assembled in a matrix $W \in \mathbb{R}^{C \times NF}$, and the objective is given by

$$F(W) = -\frac{1}{N} \sum_{i=1}^N \log \left(\frac{\exp(W_{z_i} x_i)}{\sum_{j \in C} \exp(W_j x_i)} \right), \quad (3.4)$$

where $x_i \in \mathbb{R}^{NF \times 1}$, z_i is the index of the correct class label, and $W_{z_i} \in \mathbb{R}^{1 \times NF}$ is the row vector corresponding to the weights associated with class z_i .

Figure 7 displays the performance of SGD and SQN, as measured by iteration or accessed data points, for $b = 100$ and 500 (which represent approximately 0.05%, and 0.25% of the dataset). For the SGD method, we chose the step length $\beta = 10$ for both values of b ; for the SQN method (2.9) we set $\beta = 1$. Additionally, we set $L = 20$, $M = 5$, $b_H = 1000$ in the SQN method.

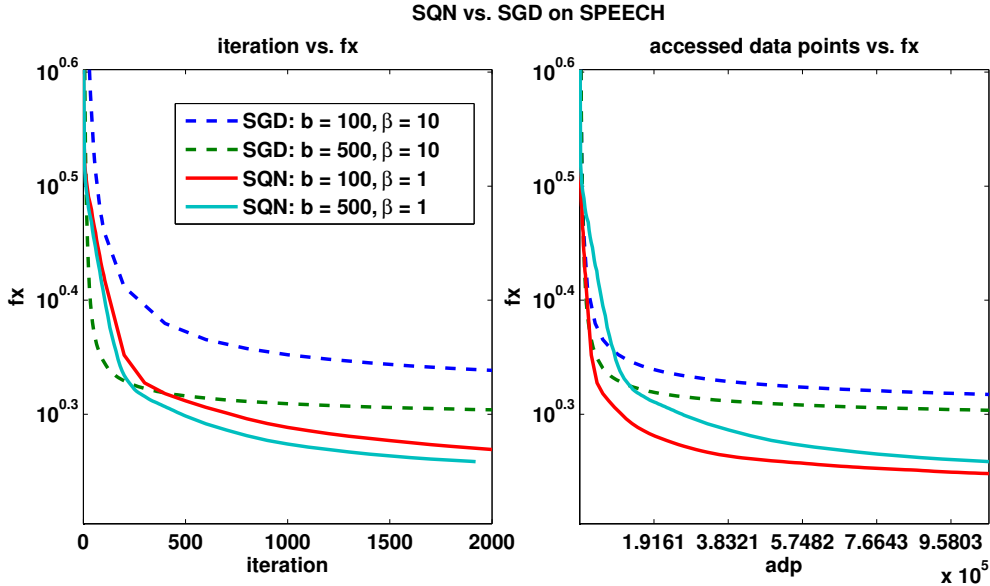


Figure 7: Illustration of SQN and SGD on the SPEECH dataset. The gradient batch size b is set to either 100 or 500, and for SQN we use $b_H = 1000$, $M = 5$ and $L = 20$. In the rightmost graph, the tick marks on the x-axis denote the epochs of the SGD method.

We observe from the figure on the right that for $b = 100$, SQN improves upon SGD in terms of adp, both initially and in finding a lower objective value. In the case of $b = 500$, SGD produces a faster initial objective decrease than SQN in terms

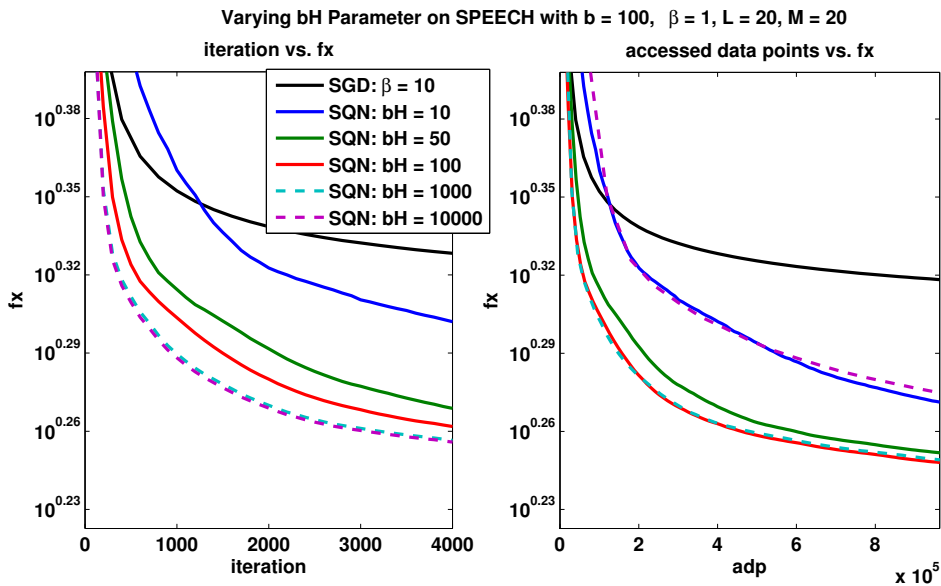


Figure 8: Varying Hessian batch size parameter b_H on SPEECH dataset. All other parameters are held constant at $b = 100$, $L = 20$, $M = 20$.

of adp, but SQN overtakes SGD after about one epoch (the first tick, 1.9161, on the x-axis of the graph on the right). Figure 7 (left) shows that the performance of SGD and SQN improves, as measured by iterations, when the batch size b is increased from 100 to 500, but for SQN this effect is smaller and is not enough to counteract the additional computational cost of the larger batch size, as shown in the rightmost figure.

The effect of varying the batch size b_H used to compute the Hessian-vector products for SQN is illustrated in Figure 8. The figure on the left shows that increasing b_H improves the performance of SQN, as measured by iterations, but only marginally from $b_H = 1000$ to $b_H = 10,000$. Once the additional computation cost of Hessian-vector products is accounted for by switching the x-axis from iterations to adp, it becomes apparent from the figure on the right that a batch size of about 100 works as well as a batch size of 1000. Once more, we observe that only a small subset of data points \mathcal{S}_H is needed to obtain useful curvature information in the SQN method.

Figure 9 illustrates the impact of increasing the memory size M from 0 to 20 for the SQN method. A memory size of zero leads to a marked degradation of performance. Increasing M from 0 to 5 improves SQN, but values greater than 5 yield no measurable benefit.

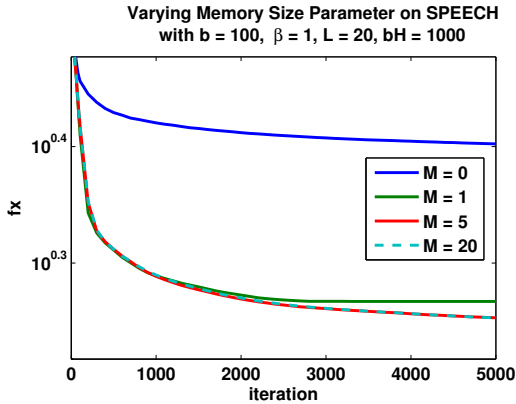
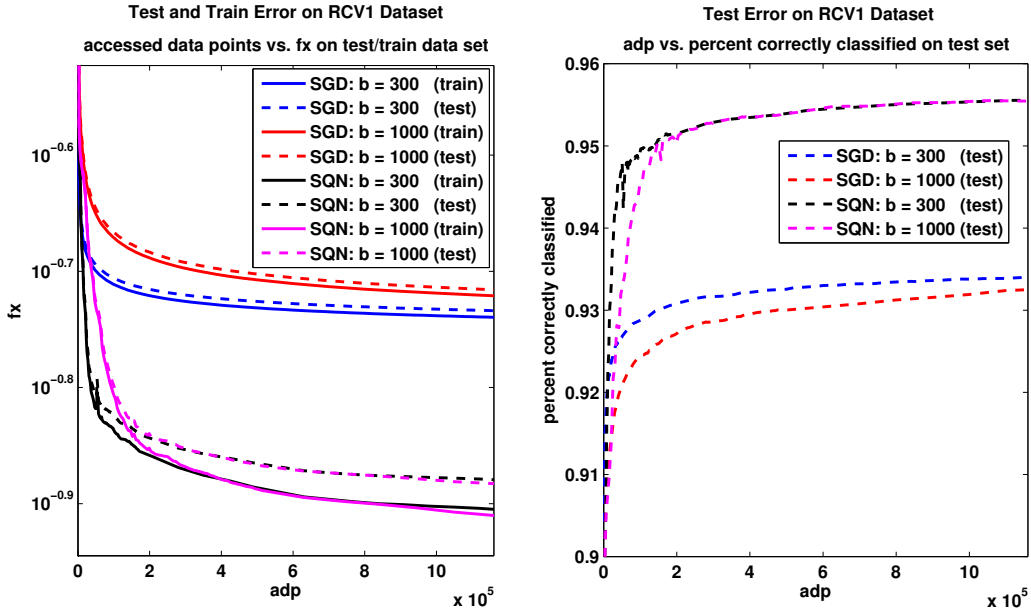


Figure 9: Performance on the SPEECH dataset with varying memory size M in the limited memory BFGS updating. All other parameters are held constant at $b = 100$, $L = 20$, $b_H = 1000$.

3.4 Generalization Error

The primary focus of this paper is on the minimization of training error (1.3), but it is also interesting to explore the performance of the SQN method in terms of generalization error. For this purpose we consider the RCV1 dataset, and in Figure 10 we report the performance of algorithms SQN and SGD with respect to unseen data (dotted lines). Both algorithms were trained using 75% of the data and then tested on the remaining 25% (the test set). In Figure 10a, the generalization error is measured in terms of decrease of the objective (3.1) over the test set, and in Figure 10b, in terms of the percent of correctly classified data points from the test set. The first measure complements the latter in the sense that it takes into account the confidence of the correct predictions and the inaccuracies wrought by the misclassifications. Recall that there are 2 classes in our RCV1 experiments, so random guessing would yield a percentage of correct classification of 0.5.

As expected, the objective on the training set is lower than the objective on the test set, but not by much. These graphs suggests that over-fitting is not occurring since the objective on the test set decreases monotonically. The performance of the stochastic quasi-Newton method is clearly very good on this problem.



(a) Training and test error on the objective (b) Test error for percent correctly classified

Figure 10: Illustration of the generalization error on the RCV1 dataset. For both SGD and SQN, b is set to 300 or 1000; for SQN we set $b_H = 1000$, $M = 5$ and $L = 20$.

3.5 Small Mini-Batches

In the experiments reported in the sections 3.2 and 3.3, we used fairly large gradient batch sizes, such as $b = 50, 100, 1000$, because they gave good performance for both the SGD and SQN methods on those problems. Since we set $M = 5$, the cost of the multiplication $H_t \widehat{\nabla} F(w^k)$ (namely, $4Mn$) is small compared to the cost of bn for a batch gradient evaluation. We now explore the efficiency of the stochastic quasi-Newton method for smaller values of the batch size b .

In Figure 11 we report results for the SGD and SQN methods for problem RCV1, for $b = 10$ and 20. We use two measures of performance: total *computational work* and adp. For the SQN method, the work measure is given by (2.13), which includes the evaluation of the gradient (1.4), the computation of the quasi-Newton step (2.9), and the Hessian-vector products (2.5).

In order to compare total work and adp on the same figure, we scale the work by $1/n$. The solid lines in Figure 11 plot the objective value vs adp, while the dotted lines plot function value vs total work. We observe from Figure 11 that, even with a small batch b , and assuming a high Hessian-vector product cost, the SQN method outperforms SGD by a significant margin. Note that in this experiment the $4Mn$ cost

of computing the steps is still less than half the total computational cost of the SQN iteration.

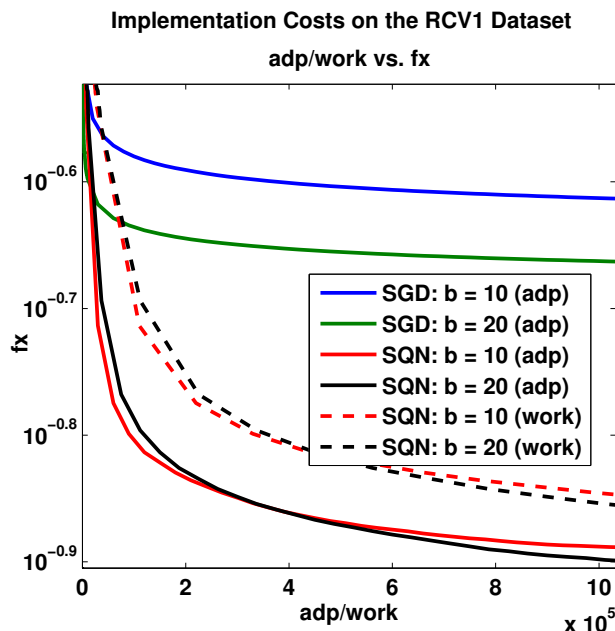


Figure 11: Comparison using $b = 10, 20$ on RCV1. The solid lines measure performance in terms of adp and the dotted lines measure performance in terms of total operation costs. For SQN we set $M = 5$, $b_H = 1000$, $L = 200$, $\beta = 1$, and for SGD we set $\beta = 5$. Note that we scale work by a factor of $1/n$.

In this experiment, it was crucial to update the quasi-Newton matrix infrequently ($L = 200$), as this allowed us to employ a large value of b_H at an acceptable cost. In general, the parameters L , M and b_H provide much freedom in adapting the SQN method to a specific application.

4 Related Work

Various stochastic quasi-Newton algorithms have been proposed in the literature [23, 13, 4, 21], but have not been entirely successful. The methods in [23] and [13] use the BFGS framework; the first employs an L-BFGS implementation and the latter uses a regularized BFGS matrix. Both methods enforce uniformity in gradient differencing by resampling data points so that two consecutive gradients are evaluated with the same sample \mathcal{S} ; this strategy requires an extra gradient evaluation at each iteration. The algorithm presented in [4] uses SGD with a diagonal rescaling matrix based on the secant condition associated with quasi-Newton methods. Similar to our approach,

[4] updates the rescaling matrix at fixed intervals in order to reduce computational costs. A common feature of [23, 13, 4] is that the Hessian approximation is updated with a relatively high level of noise.

A two-stage online Newton strategy is proposed in [3]. The first stage runs averaged SGD with a step size of order $O(1/\sqrt{k})$, and the second stage minimizes a quadratic model of the objective function using SGD with a constant step size. The second stage effectively takes one Newton step, and employs Hessian-vector products in order to compute stochastic derivatives of the quadratic model. This method is significantly different from our quasi-Newton approach.

A stochastic approximation method that has shown to be effective in practice is AdaGrad [8]. The iteration is of the form (1.5), where B_k is a diagonal matrix that estimates the diagonal of the squared root of the uncentered covariance matrix of the gradients; it is shown in [8] that such a matrix minimizes a regret bound. The algorithm presented in this paper is different in nature from AdaGrad, in that it employs a full (non-diagonal) approximation to the Hessian $\nabla^2 F(w)$.

Amari [1] popularized the idea of incorporating information from the geometric space of the inputs into online learning with his presentation of the natural gradient method. This method seeks to find the steepest descent direction in the feature space x by using the Fisher information matrix, and is shown to achieve asymptotically optimal bounds. The method does, however, require knowledge of the underlying distribution of the training points (x, z) , and the Fisher information matrix must be inverted. These concerns are addressed in [18], which presents an adaptive method for computing the inverse Fisher Information matrix in the context of multi-layer neural networks.

The authors of TONGA [22] interpret natural gradient descent as the direction that maximizes the probability of reducing the generalization error. They outline an online implementation using the uncentered covariance matrix of the empirical gradients that is updated in a weighted manner at each iteration. Additionally, they show how to maintain a low rank approximation of the covariance matrix so that the cost of the natural gradient step is $O(n)$. In [21] it is argued that an algorithm should contain information about both the Hessian and covariance matrix, maintaining that that covariance information is needed to cope with the variance due to the space of inputs, and Hessian information is useful to improve the optimization.

Our algorithm may appear at first sight to be similar to the method proposed by Byrd et al. [7, 6], which also employs Hessian-vector products to gain curvature information. We note, however, that the algorithms are different in nature, as the algorithm presented here operates in the stochastic approximation regime, whereas [7, 6] is a batch (or SAA) method.

5 Final Remarks

In this paper, we presented a quasi-Newton method that operates in the stochastic approximation regime. It is designed for the minimization of convex stochastic functions, and was tested on problems arising in machine learning. In contrast to previous attempts at designing stochastic quasi-Newton methods, our approach does not employ differences of gradients, but gathers curvature information pointwise, and feeds this information into the BFGS formula, which is entrusted with the task of computing an inverse Hessian approximation.

Our numerical results suggest that the method does more than rescale the gradient, i.e., that its improved performance over the stochastic gradient descent method of Robbins-Monro is the result of incorporating curvature information in the form of a full (i.e. non-diagonal) matrix.

The practical success of the algorithm relies on the fact that the batch size b_{hv} for Hessian-vector products can be chosen large enough to provide useful curvature estimates, while the update spacing L can be chosen large enough (say $L = 20$) to amortize the cost of Hessian-vector products, and make them affordable. Similarly, there is a wide range of values for the gradient batch size b that makes the overall quasi-Newton approach (1.6) viable.

The use of the Hessian-vector products (2.5) may not be essential; one might be able to achieve the same goals using differences in gradients, as in (2.7). This would require, however, the evaluation of gradients in (2.7) using the same batch so as to obtain sample uniformity, as well as the development of a strategy to prevent close gradient differences from magnifying round off noise. In comparison, the use of Hessian-vector products takes care of these issues automatically, but it imposes the (slightly) onerous demand of requiring code for Hessian-vector computations.

The convergence analysis of our algorithm will be the subject of a separate study. That analysis must consider the delicate interaction between noisy gradients and noisy Hessian approximations. As in any quasi-Newton method, the analysis is intrinsically complex, as the Hessian approximation influences the iterates computed by the algorithm, and these iterates in turn influence the quasi-Newton update. The generation of poor curvature estimates must be controlled, with high probability, as quasi-Newton updating is an overwriting process, and the effect of bad updates can be quite harmful.

Our numerical results suggest that the method presented in this paper holds much promise for the solution of large-scale problems arising in stochastic optimization.

References

- [1] Shun-Ichi Amari. Natural gradient works efficiently in learning. *Neural computation*, 10(2):251–276, 1998.
- [2] Søren Asmussen and Peter W Glynn. *Stochastic simulation: Algorithms and analysis*, volume 57. Springer, 2007.
- [3] F. Bach and E. Moulines. Non-strongly-convex smooth stochastic approximation with convergence rate $o(1/n)$. Technical Report 00831977, HAL, 2013.
- [4] Antoine Bordes, Léon Bottou, and Patrick Gallinari. SGD-QN: Careful quasi-Newton stochastic gradient descent. *The Journal of Machine Learning Research*, 10:1737–1754, 2009.
- [5] Leon Bottou and Olivier Bousquet. The tradeoffs of large scale learning. In J.C. Platt, D. Koller, Y. Singer, and S. Roweis, editors, *Advances in Neural Information Processing Systems 20*, pages 161–168. MIT Press, Cambridge, MA, 2008.
- [6] Richard H Byrd, Gillian M Chin, Jorge Nocedal, and Yuchen Wu. Sample size selection in optimization methods for machine learning. *Mathematical programming*, 134(1):127–155, 2012.
- [7] Byrd, R., G. M Chin, W. Neveitt, and J. Nocedal. On the use of stochastic Hessian information in unconstrained optimization. *SIAM Journal on Optimization*, 21(3):977–995, 2011.
- [8] John Duchi, Elad Hazan, and Yoram Singer. Adaptive subgradient methods for online learning and stochastic optimization. *The Journal of Machine Learning Research*, 999999:2121–2159, 2011.
- [9] R. Fletcher. *Practical Methods of Optimization*. Wiley, second edition, 1987.
- [10] Mohamed Medhat Gaber, Arkady Zaslavsky, and Shonali Krishnaswamy. Mining data streams: a review. *ACM Sigmod Record*, 34(2):18–26, 2005.
- [11] David D Lewis, Yiming Yang, Tony G Rose, and Fan Li. Rcv1: A new benchmark collection for text categorization research. *The Journal of Machine Learning Research*, 5:361–397, 2004.
- [12] D. C. Liu and J. Nocedal. On the limited memory bfgs method for large scale optimization. *Mathematical Programming*, 45:503–528, 1989.
- [13] Aryan Mokhtari and Alejandro Ribeiro. Regularized stochastic BFGS algorithm, 2013.
- [14] Indraneel Mukherjee, Kevin Canini, Rafael Frongillo, and Yoram Singer. Parallel boosting with momentum. In *ECML PKDD 2013, Part III, LNAI 8190*, pages 17–32, Heidelberg, 2013.

- [15] Noboru Murata. A statistical study of on-line learning. *Online Learning and Neural Networks*. Cambridge University Press, Cambridge, UK, 1998.
- [16] Angelia Nedić and Dimitri Bertsekas. Convergence rate of incremental subgradient algorithms. In *Stochastic optimization: algorithms and applications*, pages 223–264. Springer, 2001.
- [17] J. Nocedal and S. J. Wright. *Numerical Optimization*. Springer Series in Operations Research. Springer, second edition, 2006.
- [18] Hyeyoung Park, S-I Amari, and Kenji Fukumizu. Adaptive natural gradient learning algorithms for various stochastic models. *Neural Networks*, 13(7):755–764, 2000.
- [19] Alexander Plakhov and Pedro Cruz. A stochastic approximation algorithm with step-size adaptation. *Journal of Mathematical Sciences*, 120(1):964–973, 2004.
- [20] H. Robbins and S. Monro. A stochastic approximation method. *The Annals of Mathematical Statistics*, pages 400–407, 1951.
- [21] Nicolas L Roux and Andrew W Fitzgibbon. A fast natural Newton method. In *Proceedings of the 27th International Conference on Machine Learning (ICML-10)*, pages 623–630, 2010.
- [22] Nicolas L Roux, Pierre-Antoine Manzagol, and Yoshua Bengio. Topmoumoute online natural gradient algorithm. In *Advances in neural information processing systems*, pages 849–856, 2007.
- [23] Nicol Schraudolph, Jin Yu, and Simon Günter. A stochastic quasi-newton method for online convex optimization. 2007.
- [24] P. Tseng and S. Yun. A coordinate gradient descent method for nonsmooth separable minimization. *Mathematical Programming*, 117(1):387–423, 2009.
- [25] Farzad Yousefian, Angelia Nedić, and Uday V Shanbhag. On stochastic gradient and subgradient methods with adaptive steplength sequences. *Automatica*, 48(1):56–67, 2012.